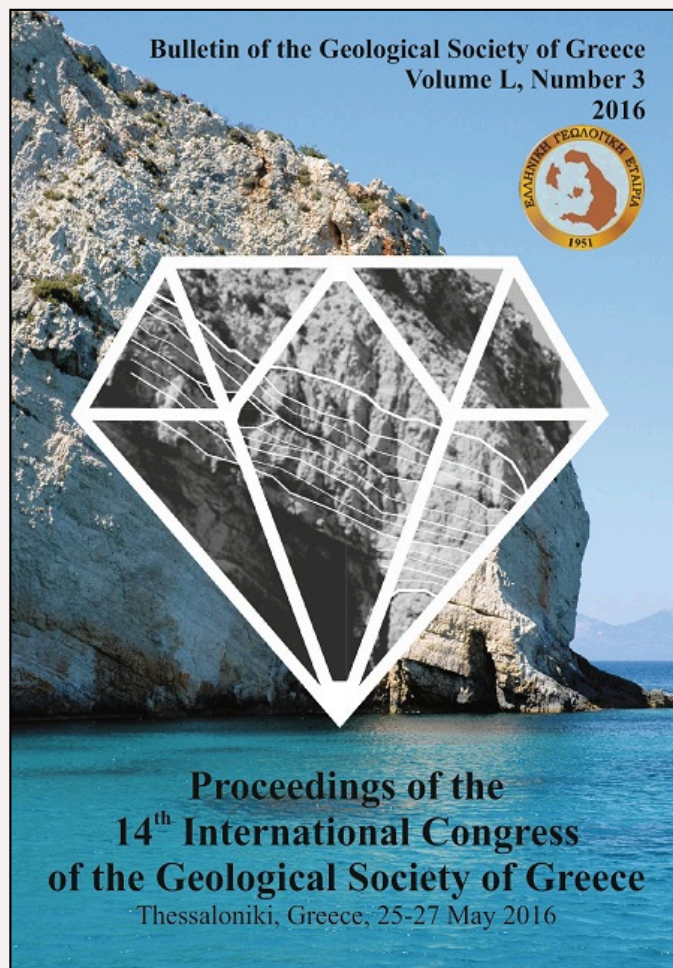


Bulletin of the Geological Society of Greece

Vol. 50, 2016



SIGNIFICANT EARTHQUAKES NEAR THE CITY OF THESSALONIKI (NORTHERN GREECE) AND PROBABILITY DISTRIBUTION ON FAULTS

Paradisopoulou P.M.

Aristotle University of
Thessaloniki, School of
Geology, Geophysics
Department

Papadimitriou E.E.

Aristotle University of
Thessaloniki, School of
Geology, Geophysics
Department

Mirek J.

Institute of Geophysics
Polish Academy of Sciences

<https://doi.org/10.12681/bgsg.11852>

Copyright © 2017 P.M. Paradisopoulou, E.E.
Papadimitriou, J. Mirek



To cite this article:

Paradisopoulou, P., Papadimitriou, E., & Mirek, J. (2016). SIGNIFICANT EARTHQUAKES NEAR THE CITY OF THESSALONIKI (NORTHERN GREECE) AND PROBABILITY DISTRIBUTION ON FAULTS. *Bulletin of the Geological Society of Greece*, 50(3), 1389-1398. doi:<https://doi.org/10.12681/bgsg.11852>

SIGNIFICANT EARTHQUAKES NEAR THE CITY OF THESSALONIKI (NORTHERN GREECE) AND PROBABILITY DISTRIBUTION ON FAULTS

Paradisopoulou P.M.¹, Papadimitriou E.E.¹ and Mirek J.²

¹Aristotle University of Thessaloniki, School of Geology, Geophysics Department 54124,
Thessaloniki, Greece, ppara@geo.auth.gr, ritsa@geo.auth.gr

²Institute of Geophysics Polish Academy of Sciences, Poland, jmirek@igf.edu.pl

Abstract

Stress triggering must be incorporated into quantitative earthquake probability estimate, given that faults are interacted through their stress field. Using time dependent probability estimates this work aims at the evaluation of the occurrence probability of anticipated earthquakes near the city of Thessaloniki, an urban center of 1 million people located in northern Greece, conditional to the time elapsed since the last stronger event on each fault segment of the study area. A method that calculates the macroseismic epicenter and magnitude according to macroseismic intensities is used to improve the existing earthquake catalog (from AD 1600 - 2013 with $M \geq 6.0$) in order to compute new interevent and elapsed time values which form the basis for time-dependent probability estimates. To investigate the effects of stress transfer to seismic hazard, the probabilistic calculations presented here employ detailed models of coseismic stress associated with the 20 June 1978 $M=6.5$ Thessaloniki which is the latest destructive earthquake in the area in the instrumental era. The combined 2015-2045 regional Poisson probability of $M \geq 6.0$ earthquakes is ~35% the regional time-dependent probability varies from 0% to 15% and incorporation of stress transfer from 0% to 20% for each fault segment.

Keywords: Intensity, interevent time, coseismic stress change.

Περίληψη

Στόχος της παρούσας εργασίας είναι η εκτίμηση της χρονικά εξαρτώμενης πιθανότητας γένεσης ισχυρών σεισμών ($M \geq 6.0$) στα ενεργά ρήγματα γύρω από την πόλη της Θεσσαλονίκης, περιοχή που στο παρελθόν έχει πληγεί από αρκετούς κατατροφικούς σεισμούς με τελευταίο αυτόν του 1978. Με τη χρήση της μεθόδου υπολογισμού μακροσεισμικού επικέντρου και μεγέθους χρησιμοποιώντας μακροσεισμικές εντάσεις και από τις μακροσεισμικές περιγραφές παλαιότερων σεισμών με $M \geq 6.0$ που έγιναν στην περιοχή τα τελευταία 500 χρόνια καταβλήθηκε προσπάθεια επαναπροσδιορισμού των εστιακών παραμέτρων των ιστορικών σεισμών με σκοπό τον υπολογισμό μέσης περιόδου επανάληψης και του χρόνου από τον τελευταίο σεισμό σ' ένα ρήγμα. Για να γίνει η εκτίμηση της πιθανότητας λήφθηκε υπόψη η μεταβολή της τάσης που προκύπτει μετά από κάθε ισχυρό σεισμό και η οποία έχει ως αποτέλεσμα να επιταχύνει ή να επιβραδύνει τη γένεση ενός επόμενου σεισμού. Ενσωματώθηκε έτσι στους υπολογισμούς της χρονικά εξαρτώμενης πιθανότητας, η μεταβολή της τάσης που προκλήθηκε από το σεισμό της 20 Ιουνίου 1978 με $M=6.5$. Η συνδυαστική πιθανότητα Poisson για τα επόμενα 30 χρόνια

(2015-2045) βρέθηκε ίση με ~35%, η δεσμευμένη πιθανότητα εκτιμήθηκε από 0% έως 15% και από 0% έως 20% με το συνδυασμό των τάσεων.
Λέξεις κλειδιά: Μακροσεισμική ένταση, περίοδος επανάλιψης, μεταβολές τάσης.

1. Introduction

The city of Thessaloniki is the second largest city in the territory of Greece surrounded by several small towns and villages. In the 20th century five $M \geq 6.0$ earthquakes occurred and since 600 A.D. nine $M \geq 6.0$ earthquakes have shaken city and its satellite settlements, causing severe damage and casualties. The most severe episode took place in 1759 ($M=6.5$) when the majority of the inhabitants abandoned the city for about two years (Papazachos and Papazachou, 2003). The 1978 earthquake ($M=6.5$) was the latest destructive one, causing the collapse of buildings and loss of life in the city and nearby villages.

Using a time dependent probability method, this work aims at the evaluation of the occurrence probability of anticipated earthquakes in the city of Thessaloniki, associated with known fault segments conditional to the time elapsed since the last strong event onto each segment. For the probability estimates an earthquake catalog as long in time is possible and the calculation of Coulomb stress changes were necessary. The historical earthquake catalog for the period between A.D. 1600 and 2014 was improved by reevaluation of the earthquake source parameters using the technique of Bakun and Wentworth (1997), for earthquakes with $M \geq 6.0$, and the regional attenuation relation of Papazachos and Papaioannou (1997) which enables better calculation of historic earthquake magnitudes from intensity values. Intervent and elapsed times were then calculated along with Coulomb stress changes due to the coseismic slip of the 1978 Stivos earthquake resulting to earthquake advances and delays onto each fault segment at a depth of 10km. The probability calculations for the next 30 and 50 years were performed and given in the form of tables and maps.

2. Earthquake catalogue

In the period between A.D. 1600 and 2014 seven $M \geq 6.0$ earthquakes occurred near Thessaloniki metropolitan area (Figure 1, table 1). Strong earthquakes are documented before 1600, back to 1 A.D. (Papazachos and Papazachou, 2003; Ambraseys, 2009), but more damage descriptions begin with the 1759 Thessaloniki earthquake. Nevertheless set the 1677 Vasilika earthquake is also included in the data set due to its proximal location to Thessaloniki, although the damage reports were limited. These observations are required for the quantitative approach to historic earthquake locations and magnitudes used here.

2.1. Methodology - Data processing

Damage descriptions for the study area were published in Papazachos and Papazachou (2003) and Ambraseys (2009) and interpreted on the Modified Mercalli intensity (MMI) scale for seven earthquakes from A.D. 1600 up to now. MMI values were assigned to about 1500 damage descriptions (608 were for 1978 earthquake). These values were used to infer M and epicentre location from MMI according to the methodology of Bakun and Wentworth (1997). The intensity attenuation relation used in this study is given by equation (1):

Table 1 – Information on source parameters of earthquakes with $M \geq 6.0$, assigned to specific fault segments, the names of which are given in the first column.

Fault name	Date	Bakun and Wentworth (1997)			Papazachos and Papazachou (2003)			Ambraseys (2009)		
		M_i	$\varphi(^{\circ})$	$\lambda(^{\circ})$	M	$\varphi(^{\circ})$	$\lambda(^{\circ})$	M	$\varphi(^{\circ})$	$\lambda(^{\circ})$
Anth1	1677	6.0 ± 0.2	40.48	23.24	6.2	40.50	23.00			
Anth2	22/06/1759	6.5 ± 0.3	40.55	23.10	6.5	40.60	22.8			
Assiros	05/07/1902	6.6 ± 0.3	40.89	22.97	6.5	40.82	23.04	6.3	40.79	23.05
Ierissos	26/09/1932	6.8 ± 0.33	40.44	23.83	7	40.45	23.86	6.8	40.50	23.80
Sohos	29/09/1932	6.4 ± 0.26	40.79	23.44	6.4	40.97	23.23	6.3	40.77	23.48
Volvi	11/05/1933	6.3 ± 0.26	40.66	23.55	6.3	40.62	23.53	6.3	40.70	23.67
Stivos	20/06/1978	6.3 ± 0.26	40.74	23.24	6.5	40.61	23.27	6.4	40.73	23.25

Equation 1- Intensity attenuation relation (Papazachos and Papaioannou, 1997)

$$M_i = [-1.26 + 0.62 \cdot (MMI_i) + 0.00328d_i + 3.28 \log(d_i)] / 1.61$$

where d_i is distance in kilometres between MMI observation and epicentre. Felt reports ($MMI < III$) were excluded and $MMI \geq III$ observations were used in the calculations. The method uses a grid search for an intensity center, thus distance in equation (1) is to a point source. The input file includes the point source (which is the center of grid search), the radius of search and the grid search spacing. The input MMI values yield an output grid of moment magnitudes and confidence intervals (RMS values for each magnitude). Outputs are highly dependent to the input parameters mainly in cases of limited MMI values (such as 1677, 1759 and 1902 earthquakes). Hence a multivariable method was developed to the existing code from Bakun and Wentworth (1997). A geographical area which is defined by the user and includes the epicenter of every earthquake in the dataset is used. Within this limited area we calculate the input parameters as follows: a) the grid center point per 0.15° , b) the radius of search for each 5km and c) the grid search spacing for every 2km. The average of the moment magnitudes yields from the inputs was chosen as the best solution.

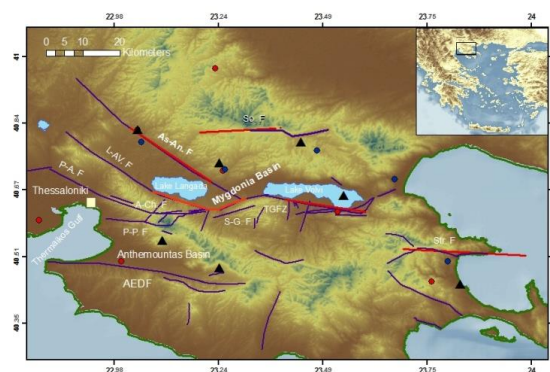


Figure 1 - Main faults of the study area (after Tranos *et al.*, 2003, So. F: Sohos Fault, As-An. F: Assiros-Analipsi Fault, L-AV. F: Lagina-Ag. Vasileio Fault, P-A. F: Pefka- svestochori Fault, A-Ch. F: Asvestochori-Chortiatis Fault, P-P. F: Pilaia-Panorama Fault, S-G. F: Stivos-Gerakarou Fault, TGFZ: Thessaloniki-Gerakarou Fault Zone, AEDF: Anthemoudas Fault). The intensity centers for each earthquake are depicted by the black triangles (Bakun and Wentworth, 1997). Red and blues circles denote the epicenters form Papazachos and Papazachou (2003) and from Ambraseys (2009) respectively.

The historical earthquake rupture most consistent with the MMI data would be the one that minimizes M and falls within 95% confidence limits on minimized misfit to input MMI values. The segment nearest to the zone of minimum magnitude of sufficient length to accommodate the historical rupture is identified as the earthquake source, with the rupture being centered in the 95% confidence interval (Figure 2).

2.2. Interevent and elapsed times

The A.D. 1600-2015 relocated earthquake catalogue comprises seven strong ($M \geq 6.0$) earthquakes (table 1, Figures 1, 2) that are used to build interevent and elapsed times for use in probability calculations. Assignment of historical earthquakes to faults indicates possible repeated rupture of some segments. The 1677, $M \sim 6.0$ and the 22 June 1759, $M \sim 6.5$ earthquakes appear to have broken two parts called Anth1, Anth2 respectively, table 1, figure 2. The 5 July 1902, $M \sim 6.6$ earthquake appears to have ruptured Assiros segment (table 1, figure 2), the 26 September 1932, $M \sim 6.8$ and the 29 September 1932, $M \sim 6.4$ earthquakes broke the Ierissos and part of Sohos faults, respectively, whereas the 11 May 1933, $M \sim 6.3$ and 20 June 1978, $M \sim 6.3$ shocks ruptured the Volvi and Stivos faults segments respectively (table 1, Figure 2). Based on the above assignment the mean earthquake interevent times (T_r) and elapsed times were found and are given in table 2. Specifically the mean interevent time was taken equal to 500 years due to limited event numbers reported for a particular fault segment, and adopting a mean return period suitable for continental faults.

Table 2 - Estimated parameters that used for probability calculations on the 7 fault segments near the city of Thessaloniki.

Fault name	T_r (years)	Elapsed Time (years)	$\dot{\epsilon}$ (bars/year)	t_a
Anth1	500	338	0.0076	50
Anth2	500	256	0.0073	50
Assiros	500	113	0.006	50
Ierissos	500	83	0.0076	50
Sohos	500	83	0.006	50
Volvi	500	82	0.0067	50
Stivos	500	37	0.0065	50

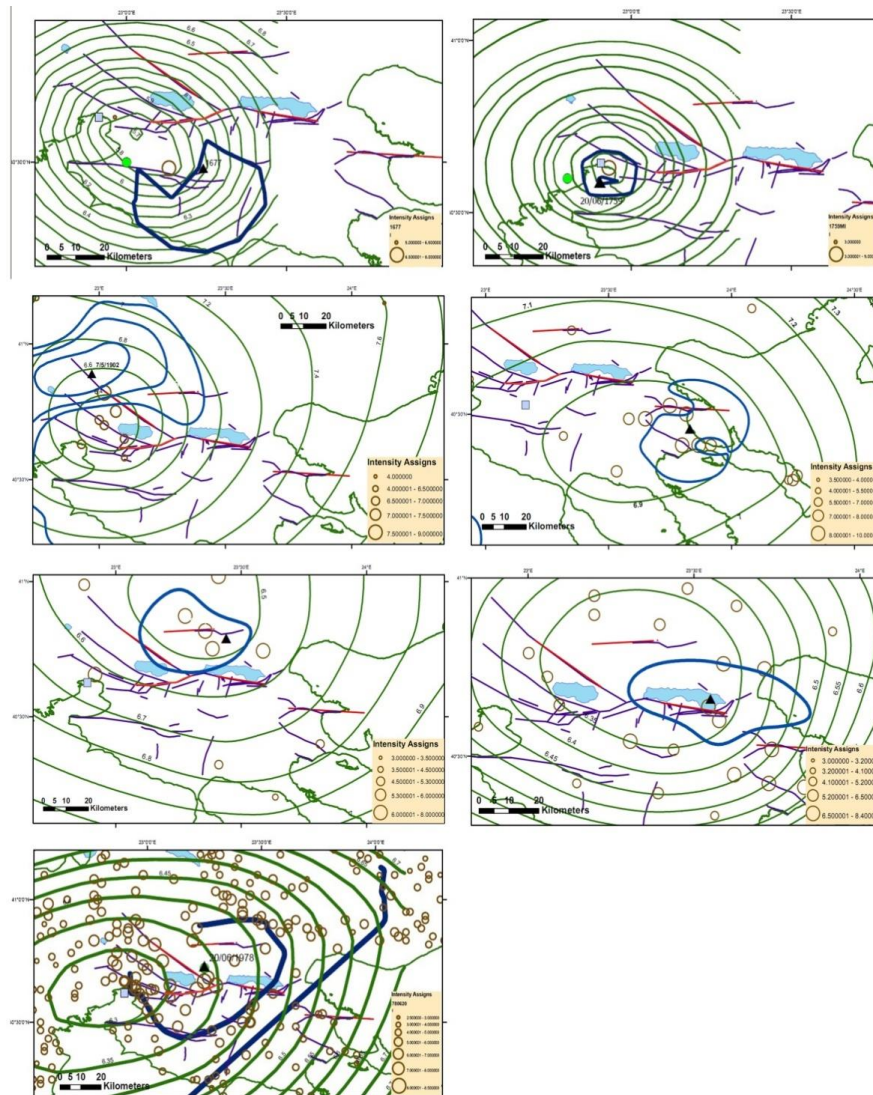


Figure 2 – Relocated earthquakes with $M \geq 6.0$ during 1600 – 2015 A.D., using MMI values estimated from damage descriptions compiled by Papazachos and Papazachou (2003). Brown circles are sites with MMI assignments with symbol size increasing with the intensity. The intensity centre shown by a black solid triangle and contours of M_i by green lines. The $\text{rms}(M_i)$ contours corresponding to the 95% confidence for location are depicted with thick blue lines.

3. Probability calculations

Occurrence probabilities for an earthquake with $M \geq 6.0$ and in the next 30 years close to the city of Thessaloniki, are calculated, onto the seven fault segments mentioned above.

3.1. Regional Poisson probability

We started with the stationary Poisson probability model which is one that treats earthquake as occurring at random in time (t) about an average interevent time T_r . The probability of at least one event in the time interval ($t, t+\Delta t$) is given by:

Equation 2- Poisson probability model

$$P(t \leq T \leq t + \Delta t) = 1 - e^{-\Delta t / T_r}$$

The estimated Poisson probabilities are given in Table 3. This model can be applied to the A.D. 16 00-2015 interevent catalog such that compined probabilities are calculated as:

Equation 3 – Combined Probability

$$P = 1 - (1 - P_{Vas.})(1 - P_{An.})(1 - P_{As.})(1 - P_{L.})(1 - P_{S.})(1 - P_{V.})(1 - P_{St.})$$

where: $P_{Vas.}$, $P_{An.}$, $P_{As.}$, $P_{L.}$, $P_{S.}$, $P_{V.}$, $P_{St.}$ are probabilities for the Vassilika, Anthemounta, Assiros, Ierissos, Sohoh, Volvi and Stivos faults, respectively. The combined 30 year probability of an earthquake to occur near the city of Thessaloniki is 34.4%.

3.2. Time dependent Probability

Earthquakes are likely not completely random in time and space as Poisson model assumes, thus time-dependent probabilities are also calculated and given in Table 3. A time-dependent probability (in any time interval ($t, t+\Delta t$)) is calculated by a probability density function $f(t)$ as (Working Group of California Earthquake Probabilities, 1990):

Equation 4 – Time dependent probability formulation

$$P(t \leq T \leq t + \Delta t) = \int_t^{t+\Delta t} f(t) dt$$

where $f(t)$ is the lognormal probability distribution (e.g. Nishenko and Buland, 1987).

3.2.1. Coulomb stress change calculations

An earthquake can be modeled as a slipping dislocation in an elastic half space (Okada, 1992) enabling estimation of stress transfer to other faults. Earthquakes occur when stress exceeds the strength of the fault. The closeness to the failure was quantified by using the change in Coulomb failure function (ΔCFF). In its simplest form, the Coulomb failure stress change is (modified from Scholz, 1990):

Equation 5 - Coulomb failure stress change formulation

$$\Delta CFF = \Delta \tau + \mu(1 - B)\Delta \sigma$$

where, $\Delta \tau$ is the change in shear stress on a fault, $\Delta \sigma$ is the change in normal stress, μ is the friction coefficient and B is the Skempton's coefficient (in this study we assume $\mu = 0.75$ and $B = 0.5$ as in Robinson and McGinty, 2000 among others). The Coulomb stress changes are calculated for 1978 earthquake, the last strong earthquake in the study area and used for earthquake probabilities estimates.

3.2.2. Incorporating stress changes from the 1978 earthquake into time dependent probability calculations

For time dependent probabilities calculations the methodology followed is that by Toda *et al.* (1998) and Parsons (2004) who support an earthquake renewal process. The probability of a future event grows as the time elapsed from the previous event increases and considering both permanent and transient effect of the stress changes. All parameters (interevent and elapsed times, tectonic stressing rate ($\dot{\epsilon}$), duration of transient effect (t_a) that used for calculations are taken from previous investigations (Paradisopoulou *et al.*, 2010, 2013) and given in Table 2.

3.2.3. Assumptions of parameters

For Coulomb stress changes calculations it is assumed that are performed in a homogeneous elastic half space and require a coefficient of friction (μ) and the Skempton's coefficient (B). One more uncertainty concerns the dip and rake angles of the target fault which are known approximately, e.g. from surface projection, or they are defined from structural information or by moment tensors or focal mechanisms. In all cases there are uncertainties that lead to variation in stress change calculations.

For probability estimations the uncertainties concern: a) the calculation of T_r and elapsed time where historical and paleoseismic data used. We try to reduce these assumptions using the Bakun and Wentworth (1997) method and recalculate the location and magnitude of historical earthquakes based on intensity assigns. b) The estimation of stressing rate $\dot{\epsilon}$ from geodetic data. The calculation of this parameter was improved using the distribution of $\dot{\epsilon}$ across and onto every fault and taking the average $\dot{\epsilon}$ value for probability estimations (Karakostas *et al.*, 2013).

For the dominant transient effect of the stress changes, rate-state constitutive relations were applied, which require parameters such as t_a (aftershock duration) and $A\sigma$ (a state parameter). We assume, according to seismicity of each subarea of the study area and the mean recurrence time (Dieterich, 1994) that t_a is equal to 10% of T_r . With given values of the parameters t_a and $\dot{\epsilon}$, the $A\sigma$ was calculated using the equation: $A\sigma = t_a \cdot \dot{\epsilon}$.

3.2.4. Results

Detailed earthquake occurrence probabilities are provided by gridding the target fault areas and performing calculations on the nodes of the grid spacing by 1km (Figures 3). The probability calculations were carried out during the next 30 (Figure 3a) and 50 years (Figure 3b) and are given in Table 3. In these figures shades of blue denote faults where the probability values are low ($0.00 \leq P \leq 0.03$) due mostly to the effect of negative changes in Coulomb stress. Shades of green and yellow represent higher probability values ($0.04 \leq P < 0.08$ and $0.09 \leq P < 0.20$, respectively) due mainly to positive ΔCFF values on these faults. The entirely blue lines represent faults that have already failed whereas orange and red lines correspond to faults that are candidate to host an incoming earthquake (higher probability values $0.20 \leq P < 0.35$).

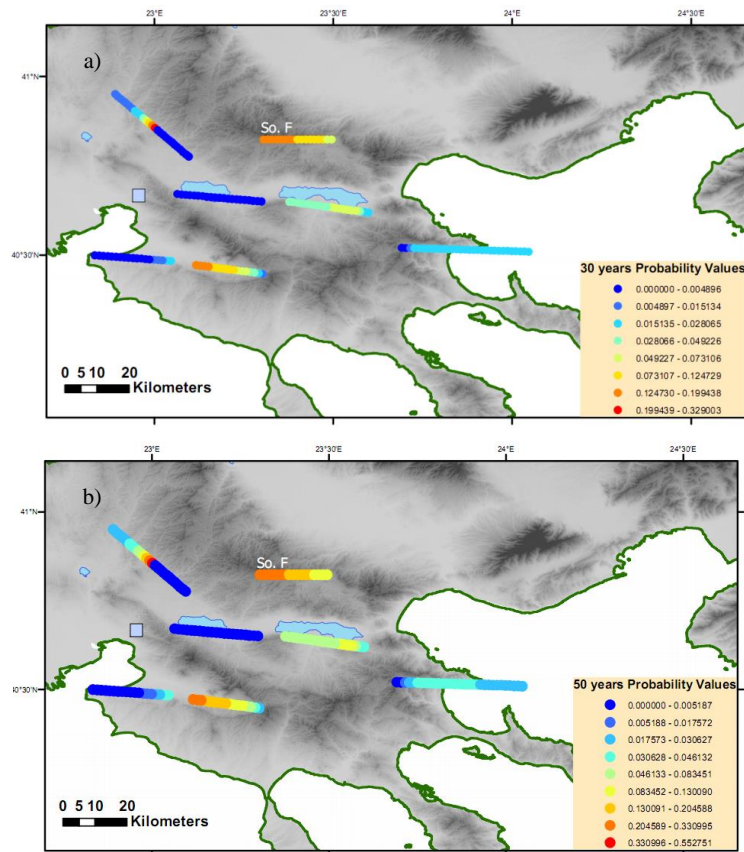


Figure 3 - Probability distribution along each fault of the study area. Colors between blue and green correspond to low probability values ($0.00 \leq P < 0.08$) whereas between yellow and red indicate higher probability values ($0.09 \leq P < 0.20$ and $P \geq 0.30$).

Table 2 - 30 and 50 years probability values (Poisson and time dependent) for the occurrence of an earthquake with $M \geq 6.0$ onto each fault segment.

Fault name	Probability before stress step				Avg ΔCFF (bars)	Probability after stress step	
	Poisson (30 yrs)	Time Dependent (30 yrs)	Poisson (50 yrs)	Time Dependent (50 yrs)		Average value [P(30)]	Average value [P(50)]
Anth1	0.06	0.09	0.095	0.15	-0.21	0.09	0.14
Anth2	0.06	0.06	0.095	0.11	-1.65	0.005	0.01
Assiros	0.06	0.01	0.095	0.02	-4.66	0.05	0.06
Ierissos	0.06	0.002	0.095	0.005	0.018	0.13	0.20
Sohos	0.06	0.002	0.095	0.005	0.15	0.02	0.03
Volvi	0.06	0.002	0.095	0.005	0.05	0.05	0.07
Stivos	0.06	0	0.095	0	-1.60	0	0

The probability of an $M \geq 6.0$ earthquake rupturing near Thessaloniki city (if a time-dependent model that includes coseismic stress changes is applied) is estimating ~10% and 13% for Anthemoundas1 and Sohos faults, respectively, in the next 30 years although the estimated probability on the same faults for 50 years is ~14% and 20% respectively. Lower probability values are found for the other five faults because of the relatively long interevent time (500 years) and because they are located inside low (negative) ΔCFF values.

4. Conclusions

Historical and instrumental records reveal that the city of Thessaloniki is frequently affected by disastrous earthquakes associated with proximal fault segments, which exhibit recurrence intervals of the order of 200 to 500 years. Intensity descriptions and attenuation relations were used in a grid search to find source locations and magnitude that best fit the intensity assignments (following Bakun and Wentworth, 1997).

The same approach was applied for the recent 1978 main shock, which served as a calibration event. The historical earthquake rupture most consistent with the MMI data would be the one that minimizes M and falls within 95% confidence bounds on minimized misfit to input MMI values. Additionally, the 1677 earthquake according to 95% confidence contour is associated with a fault segment of ~17 km in length and the 1759 earthquake with a ~20km length fault segment. The results are in accordance with active mapped faults and with fault lengths calculated from empirical relationships.

The applied method (Bakun and Wenworth, 1997) revealed that the intensity centre locations for the verification events are acceptably close to the epicentres from Papazachos and Papazachou (2003) and Ambraseys (2009). More specific for the 1978 earthquake the intensity centre is exactly at the same location with the instrumental epicentre, and for the 1759 and 1677 earthquakes the relocated epicentres are 10 and 15km, respectively, from the historical ones (table 1).

The earthquake catalogue that resulted with revised magnitudes, M_i , and intensity centre locations, enables the estimation of interevent and elapsed times necessary for probability calculations that are performed for seven faults being proximal to the city of Thessaloniki.

The Coulomb stress changes were calculated for the last strong earthquake that occurred 1978 earthquake in order to combine earthquake renewal and stress transfer into probability calculation. The ΔCFF values affect the estimated probabilities, by increasing or decreasing them when positive or negative ΔCFF values, respectively, were calculated for the particular fault segment. Thus, the probability values for an earthquake to occur for the next 30 years from 2015 on Sohos and Anthemoundas1 faults were affected from positive stress changes from the 1978 earthquake and found equal to 10% to 13%, respectively (for 50 years is ~14% and 20%, respectively). The probability estimates derived from the renewal model, as shown in Table 3, reveal that for most of the faults are smaller than those based on the Poisson model (~0.06 and 0.1). Besides, Poissonian probabilities are larger than the conditional ones due to the fact that the time elapsed since the last event of $M \geq 6.0$ onto each of the considered faults is shorter than the estimated mean interevent time.

The combined 30 year probability for the city of Thessaloniki is estimated to be equal to 34.4%.

For certain faults the differences between Poissonian and conditional estimates before the stress step are significantly different than those incorporating the stress step, and worthy to mention for future seismic hazard assessment. For the Anthemoundas and Sohos faults the Poissonian probabilities are found equal to 6% for 30 years and ~10% for 50 years, whereas the corresponding ones after the stress step are equal to 10% and 13% (for the next 30 years) and 14% and 20% for the next 50 years, respectively. The opposite consequence of ΔCFF effect is observed to the rest five faults, yielding a 30-year (50-year) Poisson of 6% (10%) and conditional probability ranging in 0.2-1%, respectively, whereas the time-dependent probabilities on these faults are from 0% to 7%.

5. Acknowledgments

All calculations concerning macroseismic data have been achieved using the Fortran code from Prof. William Bakun. The stress tensors were calculated using a program written by J. Deng (Deng and Sykes, 1997) based on the DIS3D code of S. Dunbar, which later improved (Erikson, 1986) and the expressions of G. Converse. Maps are from ArcMap tools. This work was partially supported within statutory activities No 3841/E-41/S/2015 of the Ministry of Science and Higher Education of Poland. Geophysics Department contribution 854.

6. References

- Ambraseys, N.N., 2009. Earthquakes in the Mediterranean and Middle East: a multidisciplinary study of seismicity up to 1900, ISBN 9780521872928, *Cambridge University Press*, 947 pp.
- Bakun, W.H. and Wentworth, C.M., 1997. Estimating earthquake location and magnitude from seismic intensity data, *Bull. Seism. Soc. of America*, 87, 1502-1521.
- Deng, J. and Sykes, L.R., 1997. Evolution of the stress field in southern California and triggering of moderate-size earthquakes: A 200-year perspective, *Journ. of Geophys. Res.*, 102, 9859-9886.
- Dieterich, J.H., 1994. A constitutive law for rate of earthquake production and its application to earthquake clustering, *Journal of Geophysical Research*, 99, 2601-2618.
- Erikson, L., 1986. User's manual for DIS3D: A three-dimensional dislocation program with applications to faulting in the Earth, Master's Thesis, Stanford Univ., Stanford, Calif., 167 pp.
- Karakostas, V., Papadimitriou, E., Xueshen, J., Zhihui, L., Paradisopoulou, P. and Zhang, H., 2013. Potential of future seismogenesis in Hebei Province (NE China) due to stress interactions between strong earthquakes, *Journal of Asian Earth Sciences*, 75(1-12).
- Nishenko, S.P. and Buland, R., 1987. A generic recurrence interval distribution for earthquake forecasting, *Bull. Seism. Soc. of America*, 77, 1382-1399.
- Okada, Y., 1992. Internal deformation due to shear and tensile faults in a half space, *Bull. of Seism. Soc. of America*, 82, 1018-1040.
- Papazachos, C.B. and Papaioannou, Ch.A., 1997. Macroseismic field of the Balkan area, *Journal of Seismology*, 1, 181-201.
- Papazachos, B.C. and Papazachou, C., 2003. The earthquakes of Greece, Ziti publications, Thessaloniki, 289 pp.
- Parsons, T., 2004. Recalculated probability of $M \geq 7$ earthquakes beneath the Sea of Marmara, Turkey, *Journal of Geophysical Research*, 109, doi: 10.1029/2003JB002667.
- Paradisopoulou, P., Papadimitriou, E., Mirek, J. and Karakostas, V., 2013. Coseismic stress distribution along active structures and their influence on time dependent probability values, *Bull. of the Geol. Soc. Greece*, XLVII.
- Paradisopoulou, P.M., Papadimitriou, E.E., Karakostas, V.G., Lasocki, S., Mirek, J. and Kilias, A., 2010. Influence of stress transfer in probability estimates of $M \geq 6.5$ earthquakes in Greece and surrounding areas, *Bull. Geol. Soc. Greece*, XLIII, 2114-2124.
- Robinson, R. and McGinty, P.J., 2000. The enigma of the Arthur's Pass, New Zealand, earthquake. 2. The aftershock distribution and its relation to regional and induced stress fields, *Journal of Geophysical Research*, 105, 16139-16150.
- Scholz, C., 1990. The mechanics of earthquakes and faulting, Cambridge University Press, Cambridge, 439 pp.
- Toda, S., Stein, R.S., Reasenber, P.A. and Yoshida, A., 1998. Stress transferred by the 1995 Mw=6.9 Kobe, Japan shock: Effect on aftershocks and future earthquake probabilities, *Journal of Geophysical Research*, 124, 439-451.
- Tranos, M.D., Papadimitriou, E.E. and Kilias, A.A., 2003. Thessaloniki-Gerakarou Fault Zone (TGFZ): the western extension of the 1978 Thessloniki earthquake fault (Nothern Greece) and seismic hazard assessment, *J. Struct. Geol.*, 25, 2109-2123.
- Working Group on California Earthquake Probabilities (WGCEP), 1990. Probabilities of large earthquakes in the San Francisco Bay region, *California, U.S. Geol. Surv.*, Circ. 1053, 51.